Microsyst Technol (2010) 16:585–593
DOI 10.1007/s00542-009-0970-7

TECHNICAL PAPER

Mechanical behavior of metallic glasses Mg–Cu–Y using nano-indentation

C. T. Pan · T. T. Wu · J. K. Tseng · C. Y. Su · W. J. Wang · J. C. Huang

Received: 10 October 2009 / Accepted: 30 November 2009 / Published online: 16 December 2009

Abstract The mechanical properties of amorphous bulk metallic glassy (BMG) alloy, $Mg_{58}Cu_{31}Y_{11}$, are examined using nano-indentation scratching test. This study investigates the influences of different scratching conditions on the mechanical properties such as the friction force and the friction coefficient (μ) to understand the abrasive behavior of the BMG. The scratching conditions include applied normal load, depth of scratch, scratching velocity, and scratching temperature. The experimental results of the friction force, friction coefficient, hardness, and scratching morphology of BMG are characterized. The result shows that the friction force is nearly proportional to the normal load; and the friction force exhibits a slightly dependent on the scratching temperature. Then, regression analysis method is utilized to establish a formula to fit the scratching condition of BMGs. The regression analysis can be applied to model the mathematical relationship between the scratching parameters. The regression result shows a good agreement with experimental one.

C. T. Pan · T. T. Wu · W. J. Wang
Department of Mechanical and Electro-Mechanical Engineering, Center for Nanoscience and Nanotechnology, National Sun Yat-Sen University, Kaohsiung 804, Taiwan, ROC

J. K. Tseng
Department of Mechanical Engineering, R.O.C. Military Academy, Kaohsiung, Taiwan, ROC

C. Y. Su (✉)
Institute of Manufacturing Technology, National Taipei University of Technology, Taipei 106, Taiwan, ROC
e-mail: cysu@ntut.edu.tw

J. C. Huang
Institute of Materials Science and Engineering, Center for Nanoscience and Nanotechnology, National Sun Yat-Sen University, Kaohsiung 804, Taiwan, ROC

1 Introduction

In the emerging field of nanotechnology, the manufacturing methods of nano-structures have been studied widely. The mechanical and thermal properties are important for those researches on nano-structure manufacturing. There were many methods proposed for measuring the mechanical properties. Researchers were more concerned with wear resistance of materials to predict the service life of a component and/or device. The nano-scratch test can be applied to evaluate the scratch resistance of a film surface at a low load (Li and Bhushan 1999). However, numerous other factors such as geometry of contact, velocity of sliding, lubricant and surface roughness can be equally important in affecting the tribological behavior of a material system (Ducret et al. 2003).

Bulk metallic glassy (BMG) alloys have been extensively investigated because they exhibit attractive properties such as high strength and hardness, superior corrosion resistance as well as good magnetic properties. The amorphous structures of BMG materials lead to new combinations of properties for various engineering applications. For example, it was reported that BMG provided low friction coefficient and high wear resistance (Inoue 2000; Fu et al. 2001). In recent years, Mg-based BMG matrix composites with observable plastic strains have been studied (Xu et al. 2005; Gun et al. 2006).

Glassy alloy can be applied to make magnetic head as it exhibits good wear resistance (Kohmoto et al. 1989). Liang et al. studied nano-scratch behavior of Zr-based metallic glass. Their result revealed that the part crystallization with nano-crystalline particles had good wear property (Liang et al. 2004). There were some investigations on the wear properties of BMG. Some results indicated that the metallic glass had a better wear property than the crystalline alloy

with the same composition (Long et al. 2007; Tam and Shek 2004a, b; Bhushan and Koinkar 1994). Study has been reported that metallic glasses exhibited promising tribological and wear-resistant properties (Zhang et al. 2008). Some BMG had tensile strength up to 1000 MPa with a good corrosion resistance, reasonable toughness, low internal friction and good processability (Zheng et al. 2007; Busch et al. 1998). In addition, some studies have revealed that metallic glasses showed a higher wear resistance than its crystallized state (Li et al. 2002; Thierry 2003). There were also reports indicating that the wear performances of metallic glasses were significantly inferior to the annealed state and traditional crystalline alloys (Peter and Matthew 2000).

In this study, the mechanical properties of the amorphous BMG alloy, $Mg_{58}Cu_{31}Y_{11}$, are examined by a nano-indentation scratch system (The Nano-Indenter XP system from MTS in USA). It can deliver a controlled low normal load to the tip and measure a precise movement of the tip relative to the scratched film. A lateral force measurement (LFM) module attached in the system allows the tip to move on the surface of the film, accompanied by applying loads in the range of mN. In order to better understand the abrasive action of the BMG. In this paper, a review of theoretical models applicable to scratch testing is given. The current work investigates empirically of the mechanical properties of BMG such as friction force and friction coefficient by nano-indentation scratch test. Different scratch parameters including applied normal load, depth of scratch, scratch velocity, and scratch substrate temperature are taken into consideration to investigate their effects on the mechanical properties. And then, regression analysis method is used to establish BMG scratch fitting formula. The experimental data are used to verify the regression model. In addition, the characterization of the scratch resistance and scratch deformation behavior of the $Mg_{58}Cu_{31}Y_{11}$ BMG are realized. The morphology of the surface of samples is examined by using scanning electron microscopy (SEM) and atomic force microscope (AFM).

2 Theoretical analysis

2.1 Critical depth of cut

As reported by Misra and Lal (1977), they proposed a critical depth of cut which showed the transition from ploughing to cutting by considering the theory of metal rolling. Based on this concept, the relationship between the critical depth "d" and the edge radius "R" of the tool at the onset of chip formation is given by (Gorana et al. 2006),

$$d = R(1 - \cos\theta) = 0.293R \tag{1}$$

where θ denotes the critical depth of cut at which transition starts from ploughing to cutting. This concept can be applied to nano-indentation scratch test considering spherical abrasive grain as a tool. The schematic illustration is shown in Fig. 1. Thus, the critical depth at the onset of chip formation can be estimated.

2.2 Indentation hardness

In the nano-indentation technique, hardness and Young's modulus can be determined by the method by Oliver and Pharr (1992), where the indent hardness H_m can be defined as,

$$H_m = \frac{P_{\max}}{A} \tag{2}$$

$P_{\max}$ is a maximum applied normal load, and A is the top-viewed projected area at maximum load. Figure 2 shows a typical load–displacement curve, showing the values used in the Oliver and Pharr method and cross-section of an indent during indentation. In nano-indentation, the reduced modulus "E_r" is given by,

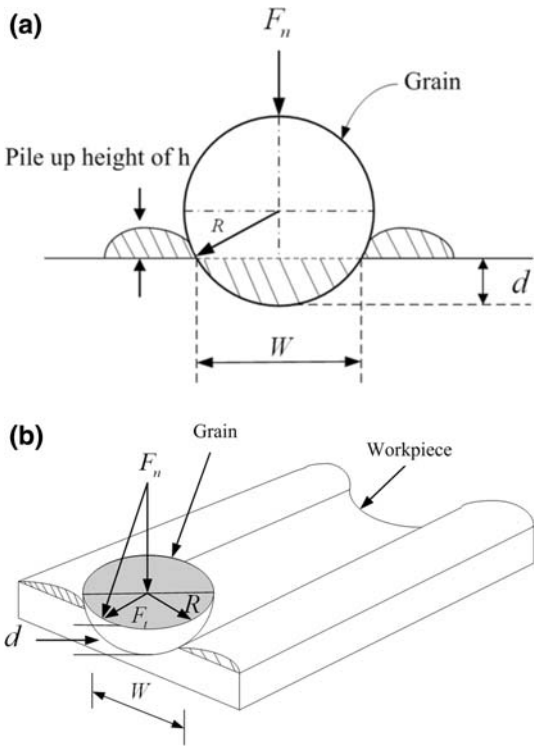

Fig. 1 **a** Indentation of a grain into the workpiece with side pile-up and **b** hemisphere normal to the direction of motion (Gorana et al. 2006)

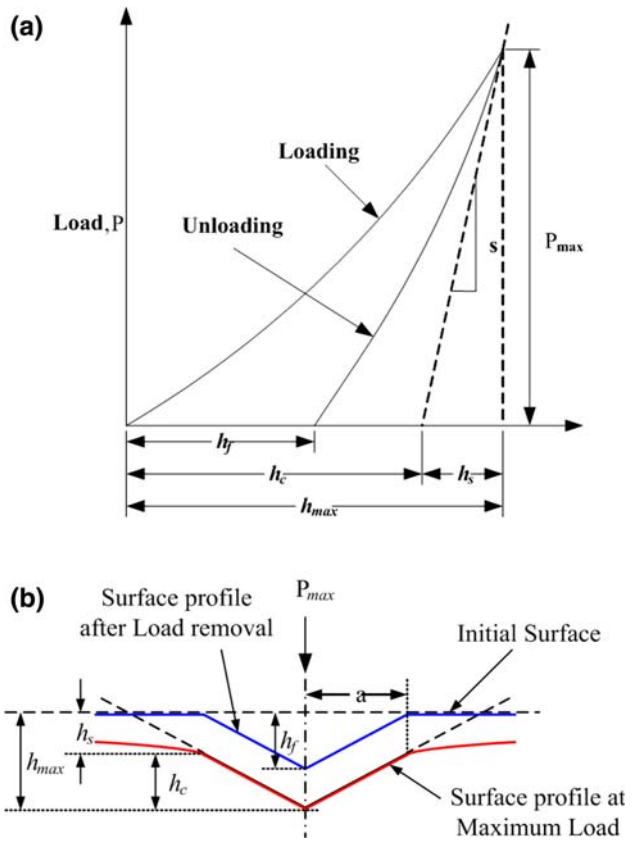

Fig. 2 **a** Load–displacement curve, showing the values used in the Oliver and Pharr method and **b** cross-section of an indentation

$$E_r = \frac{S\sqrt{\pi}}{2\beta\sqrt{A}} \tag{3}$$

The applicability of Eq. (3) to any indenter geometry has been discussed by Pharr et al. (1992) and a recent study by Schuh and Nieh (2003) has suggested that Eq. (3) is even more broadly applicable than previously thought, applying to elastic–plastic as well as purely elastic contact, where $\beta = 1.034$ for a pyramid (King 1987).

The modulus of the indented material is obtained from the following equation:

$$\frac{1}{E_r} = \frac{1-\nu_s^2}{E_s} + \frac{1-\nu_i^2}{E_i} \tag{4}$$

where E_s and ν_s are the elastic modulus and Poisson's ratio for the sample, respectively. E_i and ν_i are elastic modulus and Poisson's ratio of the indenter, respectively. The properties of the diamond indenter are $E_i = 1141$ GPa and $\nu_i = 0.07$ (Davies 1994).

2.3 Scratch model analysis

Several scratch models proposed in the literatures are briefly discussed. Gorana et al. (2006) proposed a model describing the scratch test. When the normal load F_n is exerted during nano-scratch on a grain, it indents to a depth "d" into the substrate (see Fig. 1) with a side flow of the material. The normal force on a single grain can be estimated as,

$$F_n = H_m \times A = H_m \times \pi \times \left(\frac{W}{2}\right)^2 \tag{5}$$

where W is the scratch width (see Fig. 1), and A is the projected area, respectively. The tangential force F_t (see Fig. 1) is required to move the grain forward in a direction parallel to the surface. During scratching, the tangential force consists of two components; one is ploughing force (P'') and the other is friction force (F_R).

The force P'' is required to displace (plough) the metal from the front of the single grain and is equal to the cross-sectional area of the grooved track multiplied by the yield stress of the substrate material (Gorana et al. 2006). P'' is given by,

$$P'' = \frac{W^3}{16R} H_m \tag{6}$$

The friction force F_R between the substrate material and single grain is expressed as,

$$F_R = F_n \times \mu \tag{7}$$

Substituting Eq. (5) in Eq. (7), F_R can be rearranged as Eq. (8),

$$F_R = H_m \times \pi \times \left(\frac{W}{2}\right)^2 \times \mu \tag{8}$$

where μ is friction coefficient between substrate material and single grain.

$$F_t = P'' + F_R \tag{9}$$

Substituting Eq. (6) and (8) in Eq. (9), F_t can be expressed as,

$$F_t = \frac{W^3}{16R} H_m + H_m \times \pi \times \left(\frac{W}{2}\right)^2 \times \mu \tag{10}$$

The measured scratch width and hardness can be substituted into Eq. (8) to estimate the tangential force.

3 Experimental details

3.1 Material

$Mg_{58}Cu_{31}Y_{11}$ BMG in the rod form with a diameter of 4 mm were prepared by a copper mold injection casting technique, through the induction melting of pure Mg and pre-alloyed Cu–Y ingots in an argon atmosphere. The basic thermal properties were first measured in a continuous

heating mode by differential scanning calorimetry (DSC) and thermomechanical analyzer (TMA). The applied heating rate was 10 K/min. The amorphous sample exhibits a supercooled liquid region $\Delta T_x = (T_x - T_g) = 66$ K with the onset of the glass transition T_g at 140°C (413 K) and the onset crystallization temperature T_x at 206°C (479 K), respectively, which are obtained by DSC (Chang et al. 2007).

3.2 Process procedures

All scratch experiments were performed using a Nano-indenter XP system with LFM option (force resolution of 75 nN and displacement resolution of 0.1 nm). A Berkovich pyramid indenter was used for scratch experiment. A practical indenter has a non-zero tip radius, which is actually a sphere with a given radius.

All experimental data were designed in two groups; one group was designed for training the model, and the other was designed to verify the model. All experimental data have independent variables, which are normal load (F_n), scratch velocity (v_2), depth of scratch (h_3), test temperature (T_4) and friction force (F_R).

In this study, scratch experiments were performed at various velocities ranging from 0.5 to 150 μm/s; various substrate temperatures from 298 to 453 K, various normal loads from 5 to 475 mN; and various depth of scratch from 25 to 150 nm.

During the scratching, the friction force was continuously measured and then the scratch friction coefficient was calculated by dividing the friction force by the normal force. The cross profiles show the pile up height "h" and the scratch width "W" as shown in Fig. 3. After scratching, the scratched tracks are observed using a SEM and the scratched cross-sectional area is measured using AFM.

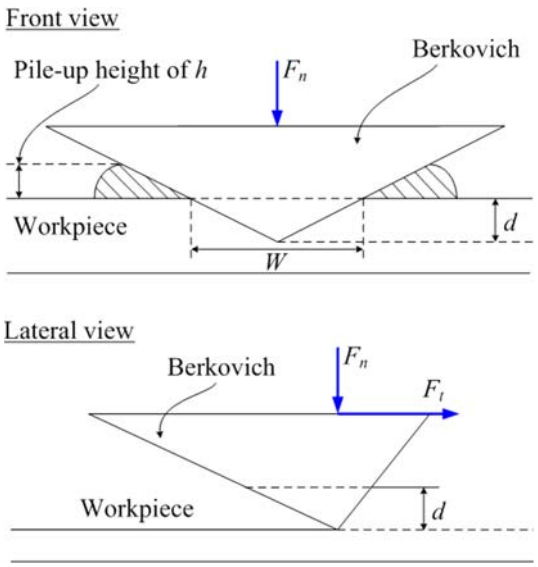

Fig. 3 Parameters describing the geometry of the nanoindentation scratch test

4 Results and discussions

4.1 Hardness measurements

In addition to the above-mentioned parameters to characterize the scratch deformation resistance, scratch hardness (H_s) is often regarded as a parameter which influences a material's resistance to scratch. The hardness was measured by berkovich indentation with a nano-indenter.

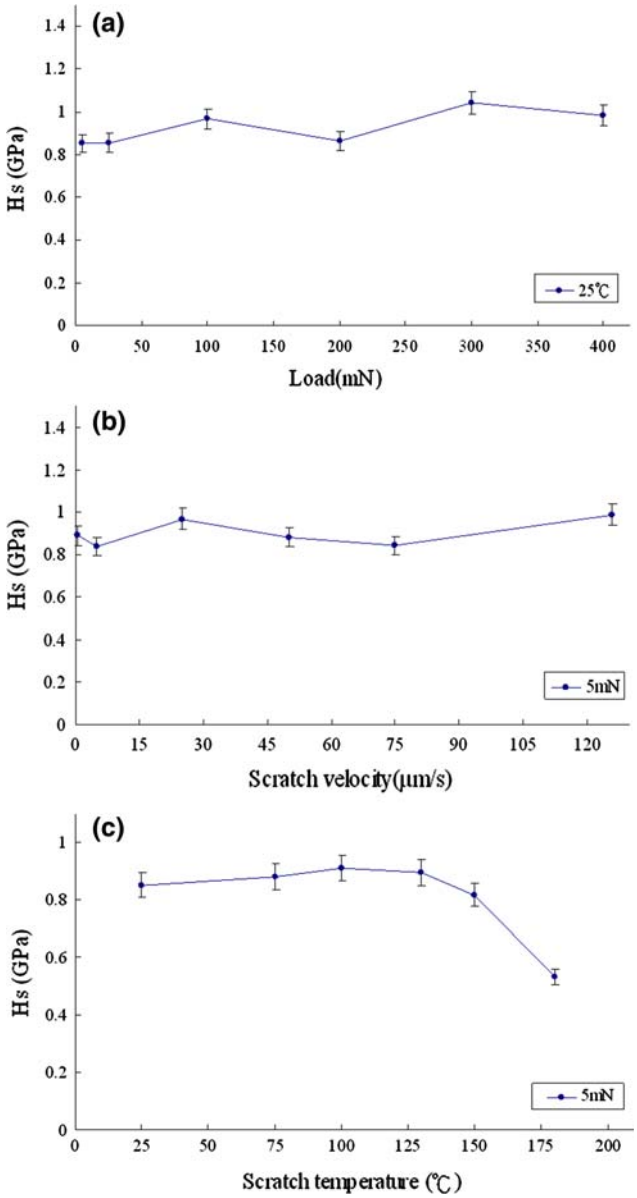

Fig. 4 The hardness as a function of the scratch conditions for BMG **a** normal load, **b** scratch velocity, and **c** scratch temperature

Figure 4a shows the experimental data for the hardness of the BMG versus the normal load. In the case of test temperatures at 25°C, the result shows that there is no obvious variation on the hardness as the load increases. Figure 4b shows the experimental data for the hardness of the BMG versus the scratch velocity. The result also shows that the scratch velocity exhibits no significant effect on the hardness as the velocity increases.

Figure 4c shows the experimental data for the hardness of the BMG versus the test temperature. After 150°C (423 K), the hardness decreases with the temperature. The hardness of the BMG is measured from 0.881 to 0.532 GPa. It reveals that the hardness of BMG decreases as the scratch temperature increases. It is due to the increase in the contact area between the indenter and the BMG surface when the temperature increases.

4.2 Variation of scratch deformation behavior and effect of various temperatures

As observed in the 3D topographic photo of the scratch using AFM in Fig. 5, the scratch morphology exhibits a groove with two pile-up pads formed by plastic flow around the indenter at various scratch conditions. It shows a micrograph of the BMG scratched at various temperatures 25°C (298 K) (see Fig. 5a) and 180°C (453 K) (see Fig. 5b). The width of each scratch track is measured. The geometric images such as width of scratch "*W*" and scratch depth "*d*" and pile-up "*h*" can be directly observed from the profile in Fig. 5.

4.3 Variation of friction force with various scratch conditions

The theoretical values of the friction forces acting on a single grain can be estimated from Eq. (8). The results of measured friction force are shown in Fig. 6a. It shows the friction force as a function of normal load, which is measured at a constant scratch velocity. It shows that the friction force increases with the normal loads. It is due to the increase in the contact area between the indenter and the BMG surface, which increases the friction force. The friction forces for various scratch temperatures and normal loads are shown in Fig. 6b. It reveals that the friction force as a function of scratch temperatures, measured at a constant scratch velocity. It can be observed that the friction force increases slightly with temperature. The friction force for different various scratch velocities and normal loads are shown in Fig. 6c. The effect of scratch velocities on the friction force is not so obvious.

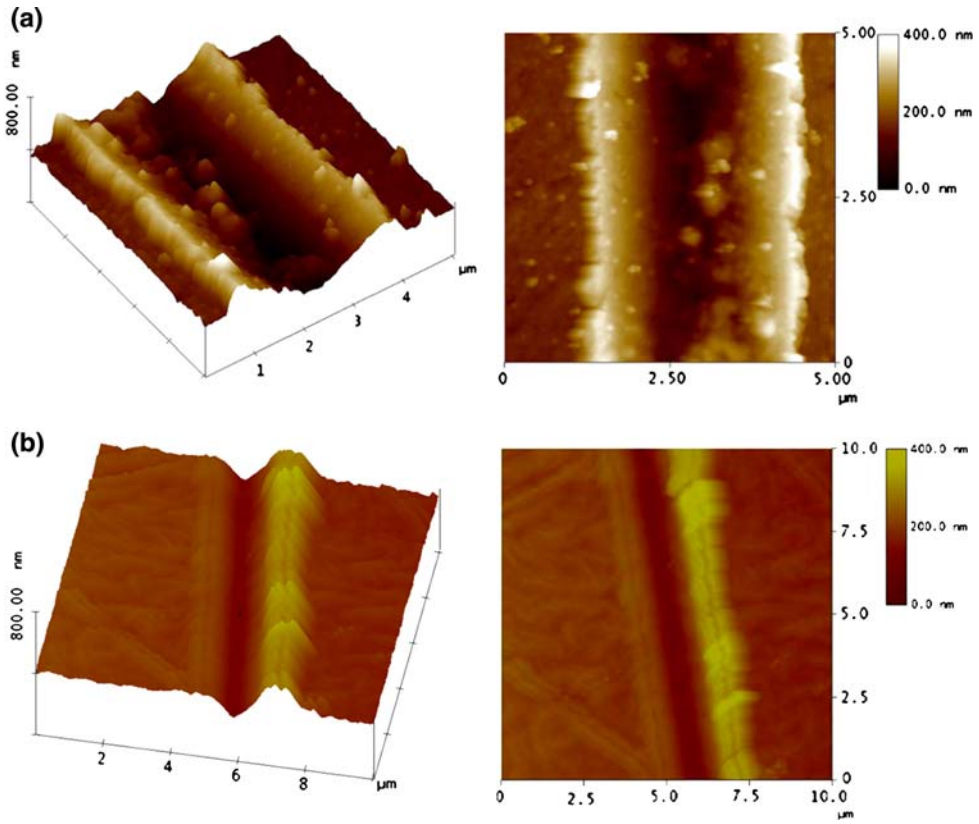

Fig. 5 AFM surface morphologies of the BMG surface and detailed 3-D scratch track images at same scratch velocity 10 µm/s and 5 mN normal load under **a** 25°C and **b** 180°C

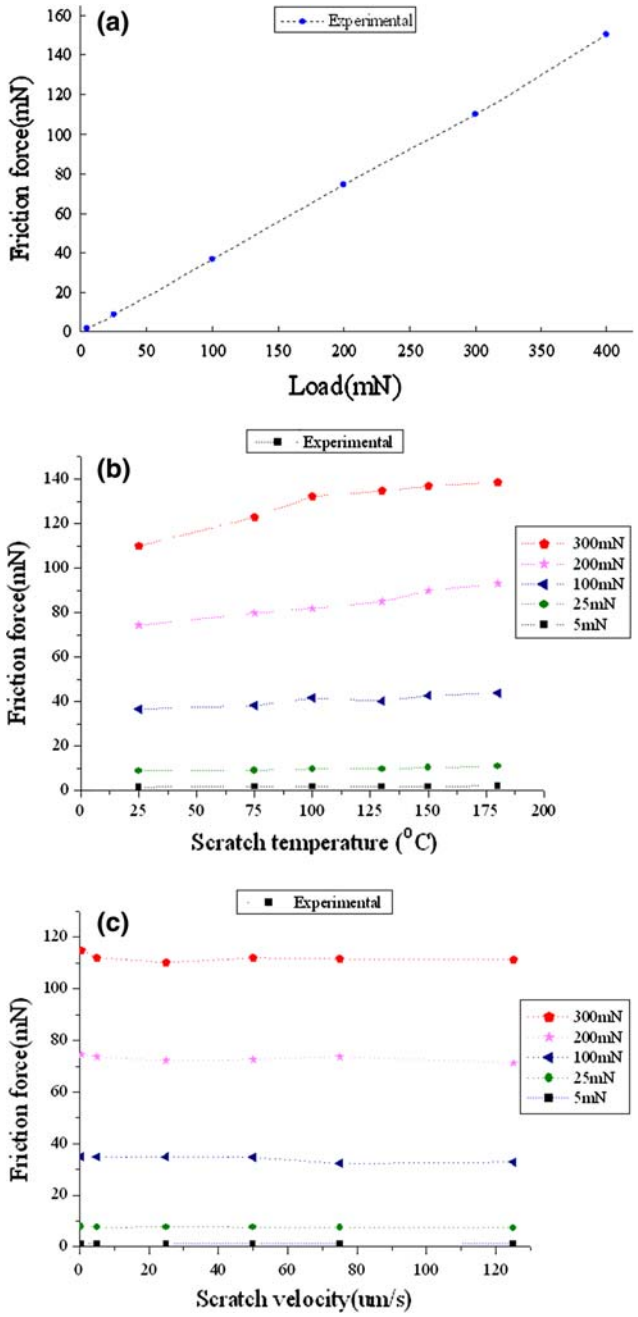

Fig. 6 Variation of friction force on a single grain with scratch parameters (**a**) normal load, (**b**) scratch temperature, and (**c**) scratch velocity

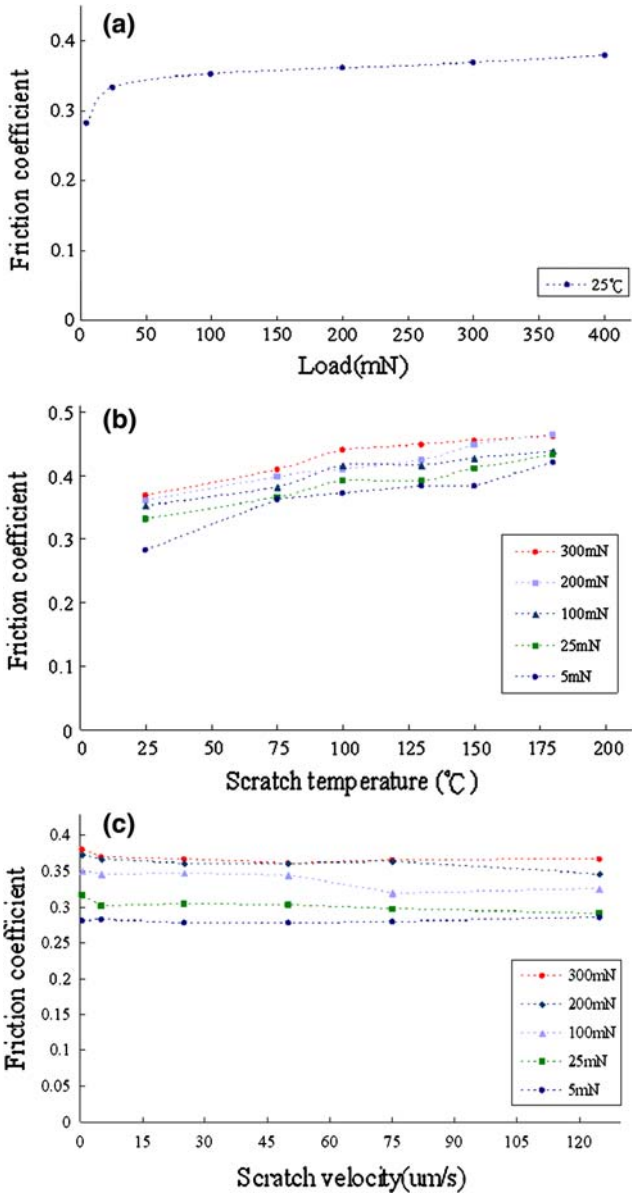

Fig. 7 Variation of friction coefficients: **a** shows the evolution of the apparent friction coefficient with normal load, **b** shows the evolution of the apparent friction coefficient with scratch temperature, and **c** shows the evolution of the apparent friction coefficient with scratch velocity

4.4 Variation of friction coefficient with various scratch conditions

Figure 7a shows the evolution of the friction coefficient with various normal loads. It shows that the friction coefficient increases with the load. It is due to the increase in the contact area between the indenter and the BMG surface, which causes the increase in friction coefficient.

Figure 7b shows the relationship between the friction coefficient and scratch temperature. It shows that the friction coefficient increases with the substrate temperature. When the temperature rises, it causes BMG softening, which increases the contact area between the indenter and the BMG surface during indent process. The friction coefficient of the BMG has a maximum value of 0.45 at 180°C (453 K). Figure 7c shows the dependence of the friction coefficient on the scratch velocity. They show no obvious effect on the friction coefficient.

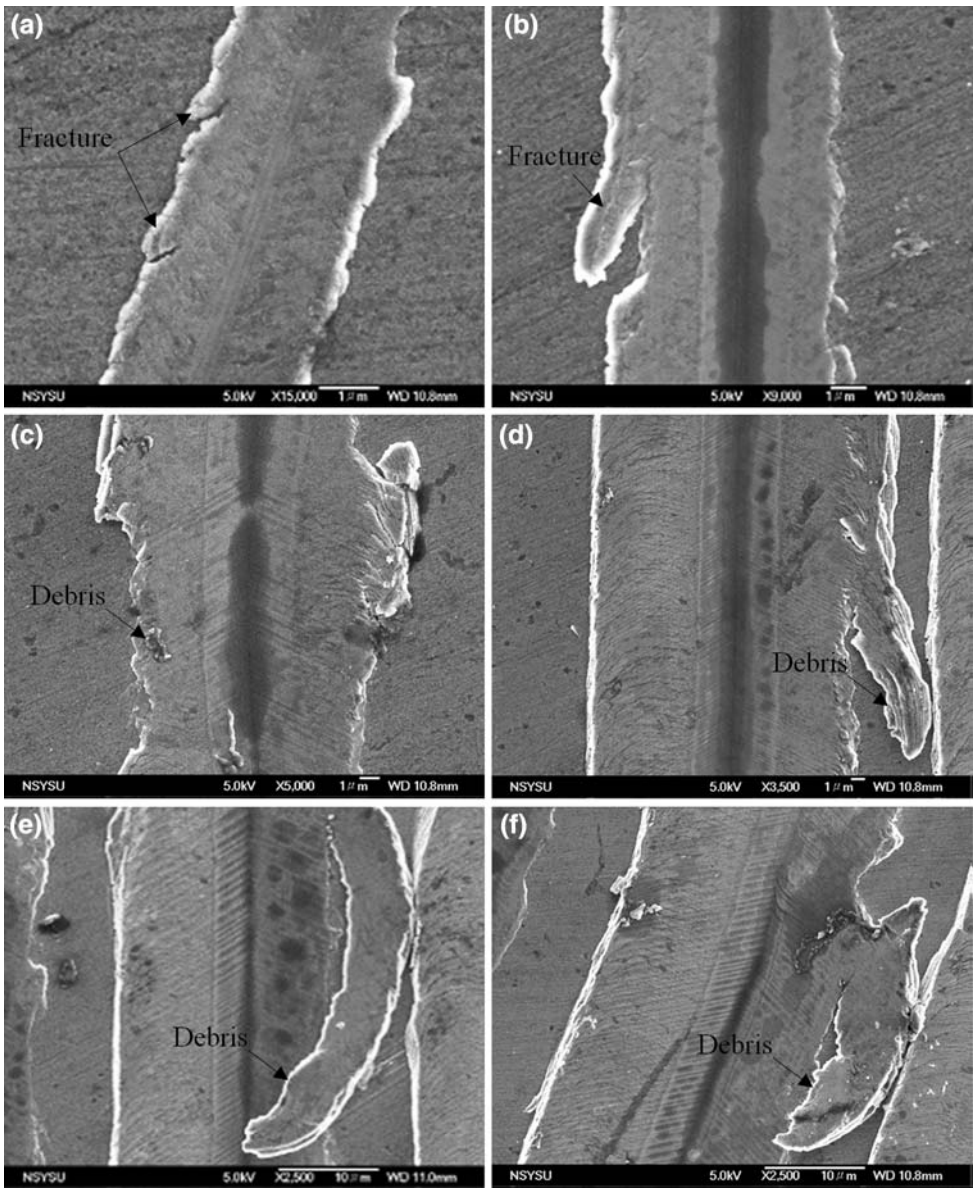

Fig. 8 SEM photographs of the BMG after nano-indentation scratch tests under the following experimental conditions: **a** 5 mN, **b** 25 mN, **c** 100 mN, **d** 200 mN, **e** 300 mN, and **f** 400 mN

4.5 Chip formation

Based on Eq. 1, the minimum critical thickness "*d*" required for chip formation is estimated. The value calculated from Eq. 1 is 11.72 nm. If scratch depth is larger than that, a chip can be produced. To discuss the value by Eq. 1, the SEM results are taken. Figure 8a shows SEM photograph of groove pattern under a normal load of 5 mN. The depth of scratch is about 25 nm. After the normal load is increased, wear debris caused by micro-fracture begins to appear on the scratch sides on the BMG surface in Fig. 8b. The more the normal loads are applied, the more the debris appears, as shown in Fig. 8c–f. From SEM photographs, it is found that the BMG surfaces usually consist of grooves and pits or pores generated by brittle fracture. Chip formation seems to occur in nanoindentation scratch test under the present scratch conditions.

4.6 Verification of the nano-indentation scratch system regression

The mathematical modeling of the nano-indentation scratch process has been carried out using a multivariable regression technique as shown in Eq. 11. This model represents the friction force in terms of normal load (F_n), scratch velocity (v_2), depth of scratch (h_3) and scratch temperature (T_4). The constants and exponents of regression equations for F_R are evaluated.

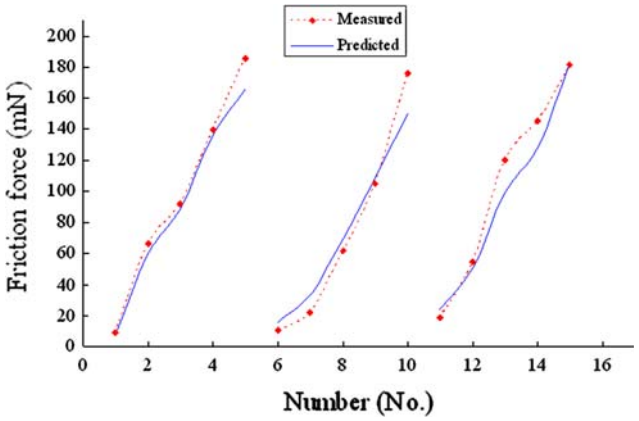

Fig. 9 The comparisons of the measured and predicted friction force

$$F_R = 0.155F_n^{1.081}v_2^{-0.006}h_3^{-0.01}T_4^{0.15} \quad (11)$$

To evaluate the performance of the developed model, 15 sets of data are used for testing. The testing data are different from the 92 sets of training data used to establish the regression models. The experimental friction force and the friction force predicted with the testing data through the regression model are compared. Figure 9 shows the comparison between the experimental and predicted friction force. It is found that the experimental result shows a good agreement with the predicted one.

5 Conclusion

During abrasive flow machining, abrasive phenomena are related to numerous factors such as geometry of contact, indenter geometry, sliding velocity, temperature and applied pressure. The influences of different scratch conditions on the mechanical properties are obtained to understand the abrasive behavior of the Mg-based BMG. The experimental results of the friction force, friction coefficient, hardness and scratched morphology of BMG are characterized as the followings: The result shows that the friction force is nearly proportional to the normal load; and the friction force exhibits a slightly dependent on the scratch substrate temperature. Then, regression analysis method is utilized to establish scratch fitting formula of BMG. The regression analysis can be applied to model the mathematical relationship between the scratch parameters to compare with experimental results.

Acknowledgments The authors would like to thank National Science Council (NSC) for their financial supports to the project (granted number: NSC95-2221-E-110-093-MY2, and NSC96-2622-E-110-010-CC3). Also, the authors would like to thank the Center for Micro/Nano Technology Research, National Cheng Kung University, Tainan, Taiwan, for equipment access and technical support.

References

Bhushan B, Koinkar V-N (1994) Nanoindentation hardness measurements using atomic force microscopy. Appl Phys Lett 64:1653–1655

Busch R, Bakke E, Johnson W-L (1998) Viscosity of the supercooled liquid and relaxation at the glass transition of the $Zr_{46.75}Ti_{8.25}Cu_{7.5}Ni_{10}Be_{27.5}$ bulk metallic glass. Acta Mater 46:4725–4732

Chang Y-C, Hung T-H, Chen H-M, Huang J-C, Nieh T-G, Lee C-J (2007) Viscous flow behavior and thermal properties of bulk amorphous $Mg_{58}Cu_{31}Y_{11}$ alloy. Intermetallics 15:1303–1308

Davies G (1994) Properties and growth of diamond. INSPEC. IEE, London

Ducret S, Mattei C-P, Jardret V, Vargiolu R, Zahouani H (2003) Friction characterization of polymers abrasion (UHWMPE) during scratch test: single and multi-asperity contact. Wear 255:1093–1100

Fu X-Y, Kasai T, Falk M-L, Rigney D-A (2001) Sliding behavior of metallic glass Part I: experimental investigations. Wear 250:409–419

Gorana V-K, Jain V-K, Lal G-K (2006) Forces prediction during material deformation in abrasive flow machining. Wear 260:128–139

Gun B, Laws K-J, Ferry M (2006) Static and dynamic crystallization in Mg–Cu–Y bulk metallic. J Non-Cryst Solids 352:3865–3887

Inoue A (2000) Stabilization of metallic supercooled liquid and bulk amorphous alloys. Acta Mater 48:279–306

King R-B (1987) Elastic analysis of some punch problems for a layered medium. Int J Solids Struct 23:1657–1664

Kohmoto O, Ohya K, Ojima T (1989) Wear-resistant magnetic head using amorphous alloy material. IEEE Trans Magn 25:4490

Li X, Bhushan B (1999) Evaluation of fracture toughness of ultra-thin amorphous carbon coatings deposited by different deposition techniques. Thin Solid Films 355–356:330–336

Li G, Wang L-M, Zhan Z-I, Sun L-L, Zhang J, Wang W-K (2002) The influence of structural relaxation on the mechanical properties of $Zr_{41}Ti_{14}Cu_{12.5}Ni_{10}Be_{22.5}$ bulk metallic glass. J Phys Condens Matter 14:11077–11080

Liang S, He J-Y, Chu W-Y, Li J-X, Sun D-B, Qiao L-J (2004) Nanowear of a Zr Based bulk metallic glass/nanocrystalline alloy. Trans Mater Heat Treat 5:1195–1199

Long Z-L, Shao Y, Deng X-H, Zhang Z-C, Jiang Y, Zhang P, Shen B-L, Inoue A (2007) Cr effects on magnetic and corrosion properties of Fe-Co-Si-B-Nb-Cr bulk glassy alloys with high glass-forming ability. Intermetallics 15:1453–1458

Misra B-K, Lal G-K (1977) Transition from ploughing to cutting during machining with blunt tools. Wear 43:341–349

Oliver W-C, Pharr G-M (1992) An improved technique for determining hardness and elastic modulus using load and displacement sensing indentation experiments. J Mater Res 7:1564–1583

Peter J-B, Matthew W (2000) Sliding friction and wear of magnesium alloy AZ91D produced by two different methods. Tribol Int 33:573–579

Pharr G-M, Oliver W-C, Brotzen F-R (1992) On the generality of the relationship among contact stiffness, contact area, and modulus during indentation. J Mater Res 7:613–617

Schuh C-A, Nieh T-G (2003) A nanoindentation study of serrated flow in bulk metallic glasses. Acta Mater 51:87–99

Tam C-Y, Shek C-H (2004a) Abrasive resistance of Cu based bulk metallic glass. J Non-Cryst Solids 347:268–272

Tam C-Y, Shek C-H (2004b) Abrasive wear of $Cu_{60}Zr_{30}Ti_{10}$ bulk metallic glass. Mater Sci Eng A 384:138–142

Thierry G (2003) Microhardness and abrasive wear resistance of bulk metallic glasses and nanostructured composite materials. J Non-Cryst Solids 316:96–103

Xu Y-K, Ma H, Xu J, Ma E (2005) Mg-based bulk metallic glass composites with plasticity and gigapascal strength. Acta Mater 53:1857–1866

Zhang G-Q, Li X-J, Shao M, Wang L-N, Yang J-L, Gao L-P, Chen L-Y, Liu C-X (2008) Wear behavior of a series of Zr-based bulk metallic glass. Mater Sci Eng A 475:124–127

Zheng Q, Cheng S, Strader J-H, Ma E, Xu J (2007) Critical size and strength of the best bulk metallic glass former in the Mg-Cu-Gd ternary system. Scripta Mater 56:161–164